Transport of a space-charge dominated electron beam in a short-quadrupole channel

S. Bernal, P. Chin, R. A. Kishek, Y. Li, M. Reiser, and J. G. Wang
Institute for Plasma Research, University of Maryland, College Park, Maryland 20742

T. Godlove
FM Technologies, Inc., Fairfax, Virginia 22032

I. Haber
Naval Research Laboratory, Washington, D.C. 20375
(Received 10 June 1998; published 31 August 1998)

Results are presented for electron beam transport experiments in a 1-m-long straight section consisting of a solenoid and five short printed-circuit quadrupoles. A linear computer code for rms envelope matching, SPOT, is used for channel design, while final simulations with more realistic elements are obtained with a $2\frac{1}{2}$D version of WARP, a particle-in-cell code. Reasonable agreement is found between calculations and the effective beam envelope obtained from pictures of the beam on a movable phosphor screen. The results validate, within experimental errors, the use of short magnetic quadrupoles for the transport of space-charge dominated beams. The straight section constitutes the prototype matching section for an electron recirculator to be built at the University of Maryland. [S1098-4402(98)00014-7]

PACS numbers: 41.85.Ja, 29.27.Eg

I. INTRODUCTION

The transport of intense particle beams is of great interest to many areas of applied science: accelerators for high-energy physics, free electron lasers, heavy-ion fusion drivers, spallation neutron sources, and medical applications, among others. Many of the beam physics issues relevant to these applications can be addressed in a low-cost way by using low-energy (<10 kV), high-current (up to 100 mA) electron beams in a university laboratory setting. Based on this idea, the University of Maryland has started the development of a small electron ring [1] to extend the on-going beam physics experiments to a much longer time scale than is currently available and to investigate new beam physics issues in circular lattices [2]. An important component of the electron ring is the injection system, consisting of a straight matching section and an inflector; the former uses dc focusing elements, while the latter employs pulsed elements for focusing and deflection into the ring. The present work reports on the first experiments related to the matching section; they provide the first bench-test results of the short printed-circuit (PC) quadrupole and the ring lattice designs. Experiments with space-charge dominated beams elsewhere have used electrostatic quadrupoles to focus single or multiple beams [3]. To our knowledge, however, no beam transport experiments to date have employed quadrupoles as short as the ones intended for the Maryland ring. The need for short quadrupoles is dictated by stringent space requirements in the electron ring lattice, a situation that may become more common for the development of new accelerators for intense beams. Although the PC quadrupoles have many advantages in design, cost, and manufacture, their dominant fringe fields, arising from their small aspect ratio, have raised concern about the possible detrimental effects on the dynamics of intense beams. Another aspect of the experiments reported here is the use of a solenoid-quadrupole system for matching. While this system suits our specific experimental needs well, it presents interesting general design issues of its own.

The paper is organized as follows: Sec. II presents the beam and FODO (alternating gradient) lattice parameters important for design calculations; Sec. III describes the experiment's physical components, from the source to the diagnostics, and summarizes the experimental procedure; Sec. IV is a brief discussion of the computer codes used for lattice design and simulations. The results and discussion are presented in Sec. V.

II. BEAM AND FODO PARAMETERS

The beam and FODO lattice parameters are summarized in Table I. "FODO lattice" refers here to the periodic geometry that is the ideal continuation of the solenoid-quadrupole matching system of the experiment (Fig. 1).

TABLE I. Beam and FODO lattice parameters.

Beam energy	4 keV
Beam current, I	17 mA
Generalized perveance, K	1.0×10^{-3}
Emittance (normalized), $\varepsilon_N = \beta\gamma\varepsilon$	8.4 mm mrad
Effective emittance[a] (4 rms), ε	67 mm mrad
Transport pipe radius	1.9 cm
Half-lattice period, $S/2$	15 cm
Quadrupole aperture/length	4.4 cm/4.4 cm

[a]M. Reiser, *Theory and Design of Charged Particle Beams* (Wiley, New York, 1994), p. 59.

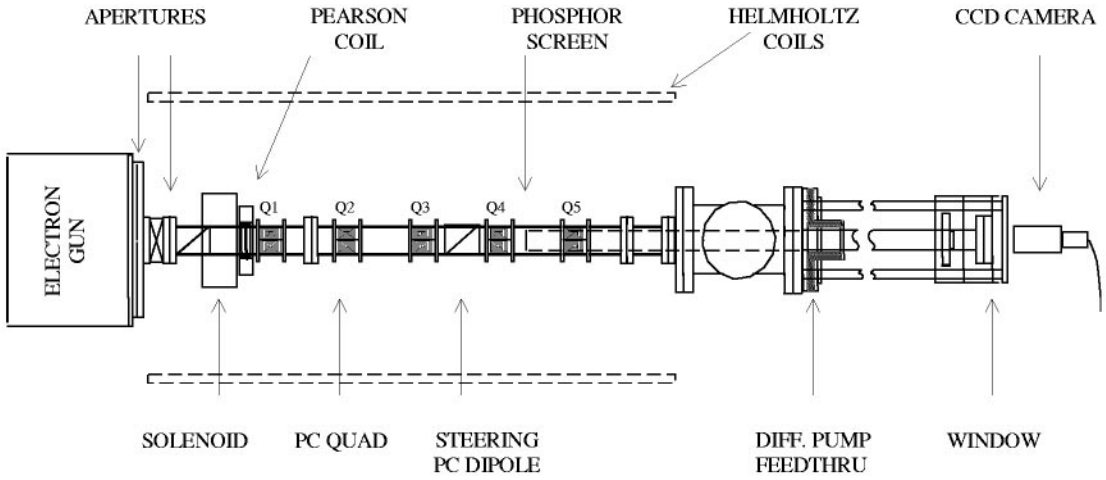

FIG. 1. Experiment setup. The PC quadrupole spacing is 15 cm.

In Table I, $K = (2I/I_0)(\beta\gamma)^{-3}$, where $I_0 = 17$ kA for electrons, and β, γ have the usual definitions in terms of the speed of light and the particle's speed. For a space-charge dominated beam $K \gg \varepsilon^2/a^2$ [see Eqs. (2) and (3) below], where a is the average beam radius in the ideal infinite FODO geometry. To a good approximation [4], $a = (S/\sigma_0)(\varepsilon\sigma_0/S + K)^{1/2}$ and $(a/a_{\max}) = (1 - 1.2\sigma_0/\pi)^{1/2}$, where σ_0 is the zero-current phase advance in the FODO lattice. These expressions yield values within about 10% of exact calculations involving Eqs. (2) and (3). In the present case, $a = 0.74$ cm (for $\sigma_0 = 85°$) and $a_{\max} = 1.13$ cm, roughly equal to the radius of the fluorescent screen used for diagnostics in the matching experiments. Using similar approximations, the tune depression σ/σ_0 in the infinite FODO lattice can be calculated to be $[1 + (KS/2\sigma_0\varepsilon)^2]^{1/2} - (KS/2\sigma_0\varepsilon) = 0.3$, within the design range for the future electron ring.

The numbers given above are of value only as a general guide in the design of the matching section. The details of the beam matching procedure in experiment and calculations are presented in the next two sections.

III. EXPERIMENT SETUP AND PROCEDURE

Figure 1 illustrates the experiment setup. The electron beam, originating about 12 cm behind the second aperture, is allowed to expand before entering the solenoid field. The solenoid transforms the initially small and rapidly expanding beam into one that can be handled with the magnetic quadrupoles. The first PC quadrupole is located near the beam waist, 11.5 cm from the middle plane of the solenoid. Four more PC quadrupoles, spaced as in the ideal FODO lattice, focus the beam to a distance of almost 1 m from the starting point. PC steering dipoles and a set of Helmholtz coils assist in beam alignment. Differential pumping allows the use of a movable phosphor screen for beam diagnostics anywhere in the channel. Details of each component are presented below.

A. Electron Gun

The first component, the electron gun, is a Pierce-type, constant perveance source which produces beam pulses in the microsecond range with energies up to about 10 keV and currents ranging from a few milliampere to about 300 mA. The gun is a scaled-down replica (2.54 cm cathode) of the SLAC klystron gun. Following the gun are two apertures used to obtain the desired current at the beam energy of the experiment. The pulse width is 5 μs and the pulse rate is 60 Hz; it is of special importance that the pulses be synchronized with nulls of the ac voltage applied to the cathode heater. This is to prevent the electron beam from acquiring significant initial angular momentum from the magnetic field of the heater coil.

B. Solenoid

The solenoid, placed 10.5 cm from the second aperture, is of the type employed in a 5 m solenoid channel used extensively for beam physics experiments at Maryland in the last 10 years [5]. The measured on-axis field of the solenoid is represented very accurately by the function

$$B_z(z) = B_0 \exp(-z^2/d^2)[\mathrm{sech}(z/b) + C_0 \sinh^2(z/b)], \quad (1)$$

where B_0 is the field in the middle plane of the solenoid and C_0, b, d are fit coefficients (see Table II). This function allows us the direct computation (through the derivatives) of the solenoid off-axis nonlinear axial and radial field components for simulations with the particle-in-cell (PIC) code discussed in Sec. IV. Furthermore, Eq. (1) makes possible the separation of linear and nonlinear terms in the calculations and is less prone to errors from approximations than a direct integration of the fields from the solenoid wires. The formula in Eq. (1) is an improvement over a simpler representation used before [6].

TABLE II. Parameters of focusing elements.

	Solenoid	PC quadrupoles
Distance from second aperture	10.5 cm	22, 37, 52, 67, 82 cm
Effective length	4.5 cm	3.35 cm
Fit coefficients d, b, C_0 [Eq. (1)]	4.82 cm, 3.43 cm, 0.017	N/A
On-axis field (gradient)	66.7 G	2.71, −5.81, 6.77, −6.12, 6.23 G/cm
Current	3.71 A	358, 767.5, 895, 809, 823 mA

C. Printed-Circuit Quadrupoles

The magnetic quadrupoles are made from flexible double-layer printed circuits; their design [7] is based on the radial linearity of the axially-integrated transverse magnetic field. The deviation of this integral from the value obtained if perfect linearity is assumed is only 0.6% at 70% of the quadrupole radius (Fig. 2a). Although this is a sound criterion for the transport of low-intensity beams, as verified in previous single-particle studies [8], it is not clear that it also applies for intense beams: The integration of the quadrupole field along the actual particle trajectory in the presence of self fields may differ significantly, especially at large radii from the axis, from the single-particle value. Thus the use of a PIC code for simulations and an experimental check are required.

Unlike more conventional quadrupole lenses, the field of the short air-core PC quads consists entirely of "fringe" fields (Fig. 2b). The measurements of the field components on a scaled-up version of the quadrupole agree well with calculations with the iron-free magnetics code MAGPC (a product of the Infolytica Corporation), as described in Ref. [7]. For realistic beam simulations with the PIC code, a three-dimensional map of the field at 1 mm intervals is used, so the full z dependence of the fields and all nonlinearities are taken into account. Table II contains the effective length and peak strengths of the solenoid and quadrupoles.

D. Steering Dipoles and Helmholtz coils

Printed-circuit steering dipoles were used after the second aperture and between quadrupoles. Also, 1-m-square Helmholtz coils (see Fig. 1) were introduced in the experiment to alleviate the effect of the Earth's magnetic field and other stray fields (e.g., from vacuum ion pumps) on the low-energy electron beam. Although no special provision was used for balancing the (smaller) horizontal component of the Earth's field, the steering dipoles produced sufficient compensation.

E. Diagnostics

The diagnostics included a Pearson transformer for beam current measurements, a 2.54 cm (diameter) fluorescent screen, and a charge-coupled device (CCD) camera (Panasonic GP-KR222) with associated hardware for video-frame capture and software for image analysis and processing. The camera has 480 lines of horizontal resolution and a 50 dB signal-to-noise ratio; it provides for iris aperture and exposure controls to prevent saturation

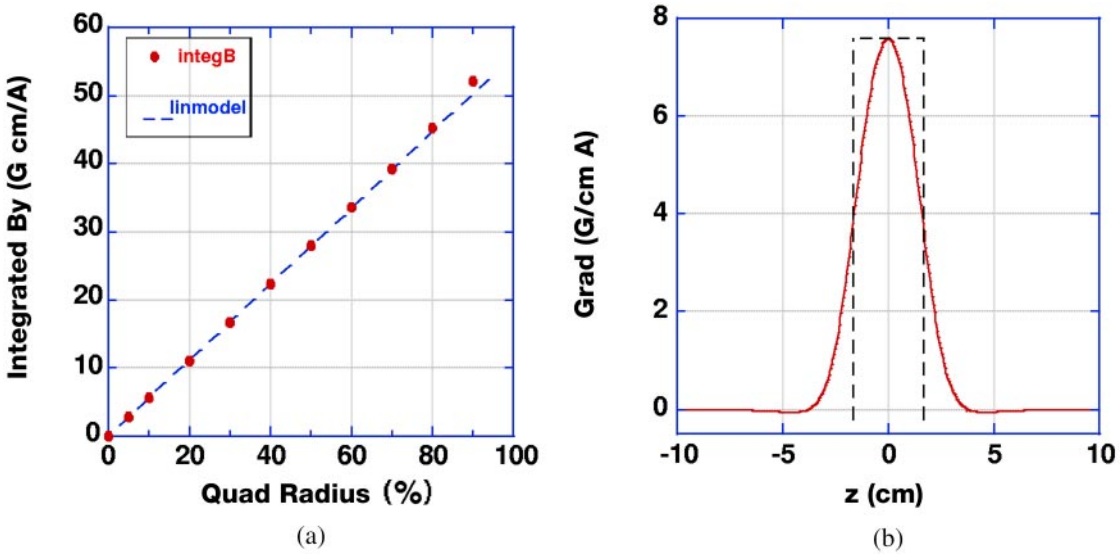

FIG. 2. (Color) PC Quadrupole: (a) radial variation of axially integrated field (per amp) at 0° and (b) on-axis gradient (per amp). The dashed lines represent the hard-top model.

of the CCD sensor (this feature is important for obtaining beam profile information). Although the phosphor screen was not calibrated (against a Faraday cup, for example) for obtaining accurate beam profiles, previous experience [9] with the relatively sharp-edged profiles of space-charge dominated beams (see Figs. 3 and 4) has shown that the uncalibrated beam profiles are, in most cases, sufficient for determining the effective beam size along the channel.

F. Experimental Procedure

The experiment proceeded in three stages. In the first step, the initial beam slope was determined from beam size data for the free expansion of the beam near the second aperture. Then, solenoid focusing was studied up to a distance of about 40 cm from the second aperture. In the last step, quadrupole focusing was observed sequentially, with special attention given to quadrupole angular placement to correct for any beam rotations relative to the quadrupole principal axes. Fortunately, rotations of the principal axes of the beam cross section arising from rotated quads are decoupled from centroid motion so they can be easily corrected in the experiment without introducing additional errors.

Beam alignment was kept within about 0.5 mm through the use of steering PC dipoles placed between quadrupoles; the Helmholtz coils mentioned above were also used for fine tuning the alignment. A final check of the alignment was done through switching of the quadrupole polarities. The alignment achieved using this method was good only in an average sense, since space allowed us only one steering dipole between quads to correct for beam centroid position at the midplane of each quadrupole.

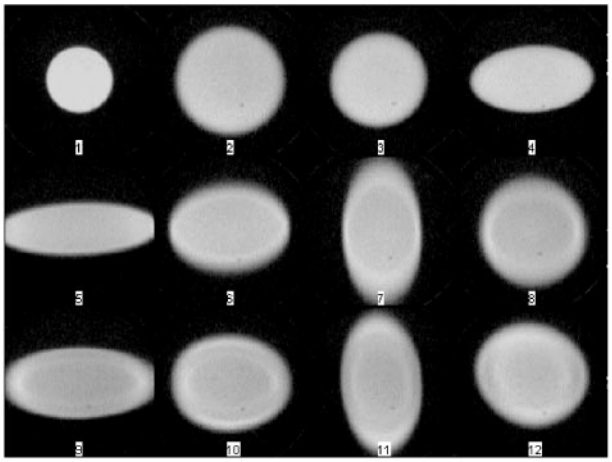

FIG. 3. Phosphor screen pictures from a CCD camera: (1) near aperture (6.3 mm diameter), near midplane of solenoid (2) and quadrupoles 1, 2, 3, 4, and 5 [(3), (5), (7), (9), and (11)]. The rest of the pictures are at planes between quads as implied.

The matched envelope solution, both in calculations and experiment, is especially sensitive to the solenoid focusing strength: A change of only 0.5% in peak solenoid field makes noticeable changes in the beam envelope. Possible displacement of the beam axis relative to the solenoid magnetic axis, as well as small hysteresis effects, affect the focusing of the solenoid. The initial beam slope and, to a lesser extent, the emittance are also important for the matched solutions. The emittance is derived from direct measurements in other experiments [9], taking into account the existence of the two apertures (Fig. 1).

A smaller role is played by the uncertainty in quadrupole currents (about 1%) and location. Finally, small errors are introduced by the use of an uncalibrated phosphor screen and noise (mostly spurious light) in the diagnostics.

IV. COMPUTER CODES

A. KV code

A preliminary study of the design of the matching section using a linear code was presented previously [10]. We review here the most important aspects of the problem.

The matching of the electron beam into an infinite FODO straight lattice is calculated using the linear code SPOT [11], which is based on the solution of the KV envelope differential equations [12]

$$X'' + \kappa_x(z)X - \frac{2K}{X+Y} - \frac{\varepsilon^2}{X^3} = 0\,, \qquad (2)$$

$$Y'' + \kappa_y(z)Y - \frac{2K}{X+Y} - \frac{\varepsilon^2}{Y^3} = 0\,, \qquad (3)$$

where X, Y are the effective beam sizes $X = 2x_{\rm rms}, Y = 2y_{\rm rms}$ in directions perpendicular to the beam propagation (z direction) and prime indicates derivative with respect to z. The other quantities, K and ε, are defined in Table I, and $\kappa_{x,y}(z)$ represent focusing functions. For particles of charge q and (design) linear momentum p_0, solenoid focusing is given by $\kappa_x = \kappa_y = [qB_z(z)/p_0]^2$, while quadrupole focusing is represented by $\kappa_x = -\kappa_y = [qg(z)/p_0]$. The on-axis solenoid field $B_z(z)$ is given by Eq. (1), while the quadrupole on-axis gradient $g(z)$ is shown in Fig. 2b.

For the matching calculations, Eqs. (2) and (3) are first solved for the beam envelopes in one period of the ideal FODO geometry (parameters of Table I) and then for the actual solenoid-quadrupole system. The strengths of all of the elements except the last one (the last quadrupole strength is kept fixed at the constant—except for sign—FODO lattice value) are varied and optimized until a solution is found (Table II). The optimization procedure does not include variations in the location of focusing elements; the locations are decided on the basis of general considerations, as discussed below, as well as simple trial and error. The integration step for the solution of the KV envelope equations is typically 0.5 mm.

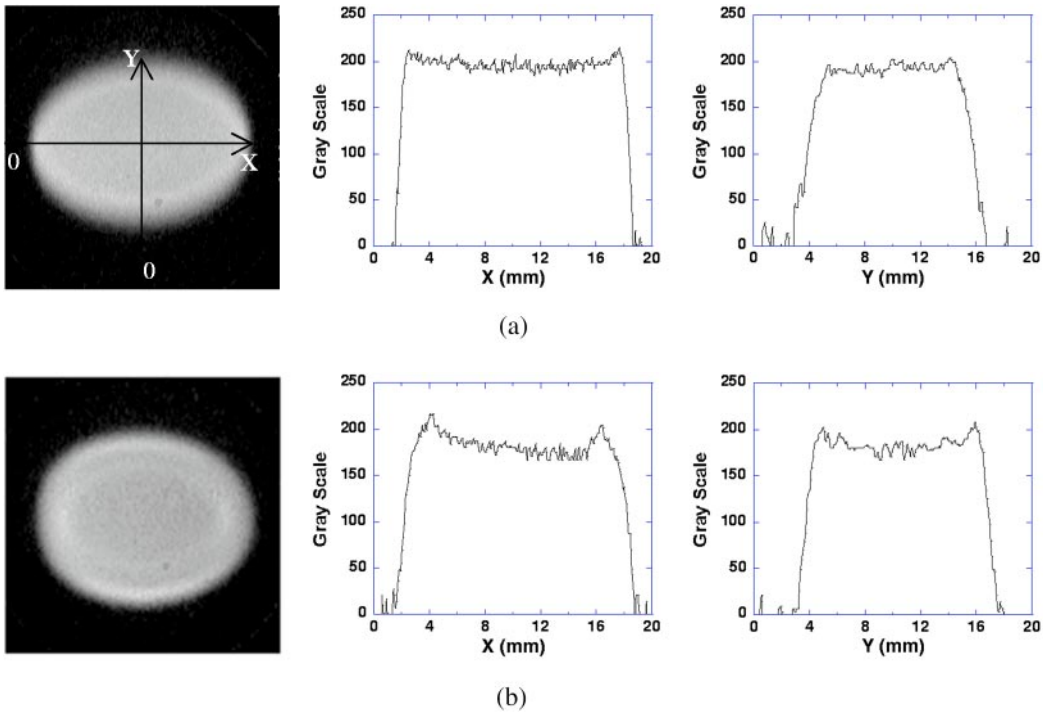

FIG. 4. (Color) Beam cross sections and density profiles near planes between quadrupoles 2 and 3 (a) and between quadrupoles 4 and 5 (b). The gray scale corresponds to an eight-bit picture, i.e., where "0" is black and "255" is white.

B. PIC code

For the PIC simulations, the single-slice version of WARP [13] was used. This version of the code runs much faster than the full 3D version: It is 2D but includes all three particle-velocity components. The single-slice code was checked against the full 3D version and found to be adequate for simulating the matching section.

The simulations with WARP start with a semi-Gaussian distribution (i.e., one with uniform particle density but nonzero transverse temperature) at the second aperture. A grid of 128×128 cells is used across the 3.8 cm of the pipe diameter, so the cell size corresponds to about $1/3$ of a Debye length. To minimize numerical collisions, 40 000 particles per slice are employed. The step size for the calculations is 2.5 mm, found to be adequate upon comparison with shorter steps.

As mentioned above, the PIC simulations employ realistic elements, including nonlinearities and z dependence. For the final simulations, the solenoid peak field, initial beam slope, and emittance are slightly adjusted within experimental errors, about nominal values, to yield the best agreement. The values given in Tables I and II reflect this adjustment.

V. RESULTS AND DISCUSSION

The beam envelope is determined experimentally from pictures taken near the middle plane of all five quadrupoles, at three more planes in between each pair of quadrupoles, and at points near the aperture. In every case, the beam sizes in the horizontal and vertical planes are calculated as twice the rms value of x and y using the pixel coordinates and gray scale values (0 to 255) as representation of the beam particle density distribution. Provisions are included in the image analysis software for noise reduction.

Figure 3 shows a partial sample of pictures taken in one run, while Fig. 4 presents typical beam profiles in the transverse directions. The internal structure observed in the beam will be the subject of a future publication.

Slight variations of the lattice geometry of Fig. 1 were tested, as well as reduced overall focusing (e.g., focusing for $\sigma_0 = 76°$ in the corresponding FODO lattice). The results are qualitatively similar for all cases, so the ones presented in the figures are representative of the experiments.

Figure 5 compares the experimental results with the numerical simulations and the KV-envelope calculations. Remarkable agreement is obtained. The close correspondence between the envelope from WARP and that predicted by the linear KV code demonstrates linear focusing of the space-charge dominated electron beam in the solenoid-quadrupole system. Furthermore, approximate rms envelope matching into a FODO lattice is achieved.

The particular lattice geometry chosen for the experiment can be understood in simple terms. The solenoid is placed at a distance such that the beam is allowed to expand to a radius roughly equal to the average radius in the

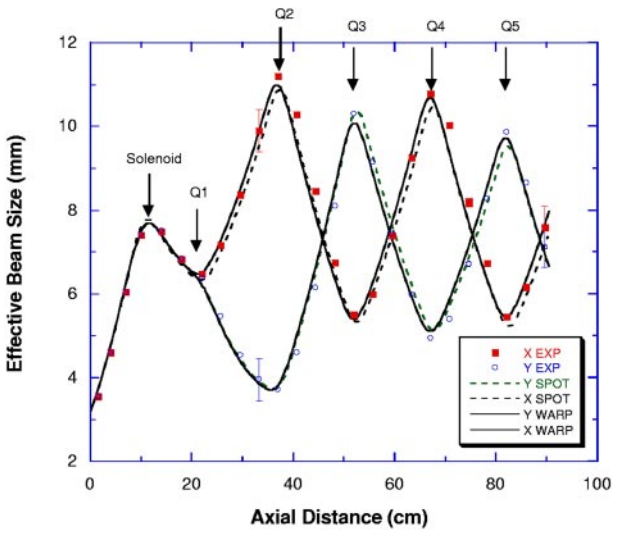

Fig. 5. (Color) Experiment vs calculations. The solid lines are results from the PIC code WARP, while the dashed lines are from the KV code SPOT. The origin on the z axis coincides with the position of the second aperture (diameter = 6.35 nm), where the beam slope is 0.032 ± 0.002 rad. The lens parameters are given in Table II.

FODO lattice. This value is small compared to the solenoid bore radius (31 mm), so the role of solenoid nonlinearities is minimized. The first quadrupole, on the other hand, is located near the beam waist; in this way the beam envelope is expected to split evenly. In practice, however, the current geometry causes an initially strong focusing of the beam in one direction, as seen in Fig. 5 (lower lobe in the envelope following the first quadrupole, Q1) and picture labeled "5" in Fig. 3. The overfocusing by Q1 can be reduced by a slight rearrangement of the lattice geometry (e.g., by moving the solenoid from $z = 10.5$ cm to $z = 12.5$ cm and changing the quadrupole strengths accordingly, following recalculations with the linear code). The new matched solutions, both measured and simulated, are otherwise like the ones shown in Fig. 5.

VI. CONCLUSION

We have used a linear code to design a matching section consisting of a short solenoid and five printed-circuit quadrupoles. The results for the effective beam size in the channel agree reasonably well with calculations in the linear model as well as with particle-in-cell simulations involving more realistic focusing elements. In this way we have shown, within the uncertainties of the experiment, that the design of small aspect-ratio magnetic quadrupoles to focus intense beams can be based on the same criteria used for zero current. Furthermore, approximate matching in a root-mean-square sense has been achieved, although internal structure observed in the beam suggests possible mismatch in the charge density profile. This latter issue will be addressed in a future publication. The results of the experiment are an important step in the development of the matching section for the University of Maryland electron ring.

ACKNOWLEDGMENTS

This research used resources of the National Energy Research Scientific Computing Center (NERSC), which is supported by the U.S. Department of Energy.

[1] M. Reiser, S. Bernal, A. Dragt, M. Venturini, J. G. Wang, H. Onishi, and T. F. Godlove, Fusion Eng. Des. **32-33**, 293 (1996).
[2] J. G. Wang *et al.*, Nucl. Instrum. Methods Phys. Res., Sect. A (to be published).
[3] M. G. Tiefenback and D. Keefe, IEEE Trans. Nucl. Sci. **32**, 2483–2485 (1985).
[4] Martin Reiser, *Theory and Design of Charged Particle Beams* (Wiley, New York, 1994), p. 385.
[5] Martin Reiser, *Theory and Design of Charged Particle Beams* (Wiley, New York, 1994), p. 484.
[6] Martin Reiser, *Theory and Design of Charged Particle Beams* (Wiley, New York, 1994), p. 224.
[7] T. F. Godlove, S. Bernal, and M. Reiser, in *Proceedings of the 1995 Particle Accelerator Conference, Dallas, Texas* (IEEE, New York, 1996), p. 2117.
[8] M. Venturini, S. Bernal, A. Dragt, M. Reiser, J. G. Wang, and T. F. Godlove, Fusion Eng. Des. **32-33**, 283 (1996).
[9] D. M. Kehne, Ph.D. thesis, University of Maryland, 1992.
[10] S. Bernal, A. Dragt, M. Reiser, M. Venturini, J. G. Wang, and T. F. Godlove, Fusion Eng. Des. **32-33**, 277 (1996).
[11] C. K. Allen, S. K. Guharay, and M. Reiser, in *Proceedings of the 1995 Particle Accelerator Conference, Dallas, Texas* (IEEE, New York, 1996), p. 2324.
[12] I. M. Kapchinskij and V. V. Vladimirskij, in *Proceedings of the International Conference on High Energy Accelerators, Geneva, 1959* (CERN, Geneva, 1959), p. 274.
[13] A. Friedman, D. P. Grote, and I. Haber, Phys. Fluids B **4**, 2203 (1992).